Supplemental Information

Title: Distinct subunit domains govern synaptic stability and synapse specificity of the kainate receptor

Christoph Straub[1, 2, #], Yoav Noam[1, 2, #], Toshihiro Nomura[3], Miwako Yamasaki[4], Dan Yan[1, 2], Herman B. Fernandes[3], Ping Zhang[5], James R Howe[5], Masahiko Watanabe[4], Anis Contractor[3], and Susumu Tomita[1, 2]

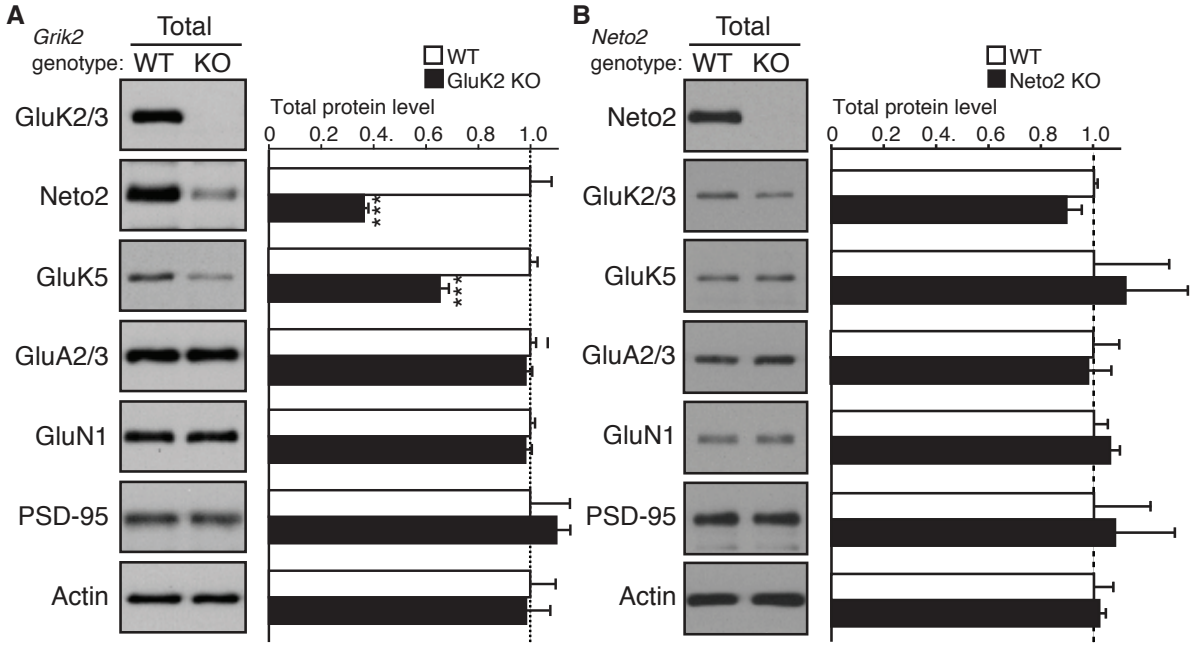

Figure S1. Total expression levels of kainate receptor components is determined by GluK2, but not Neto2, Related to Figure 1

Total protein levels in cerebellum from GluK2 KO (A) or Neto2 KO (B) mice. Levels of the kainate receptor subunits GluK2, GluK5, and Neto2 were reduced in GluK2 KO mice, but not in Neto2 KO mice (n = 4 each). Data are given as mean ± s.e.m.; ***, $P < 0.001$ (Student's t-test).

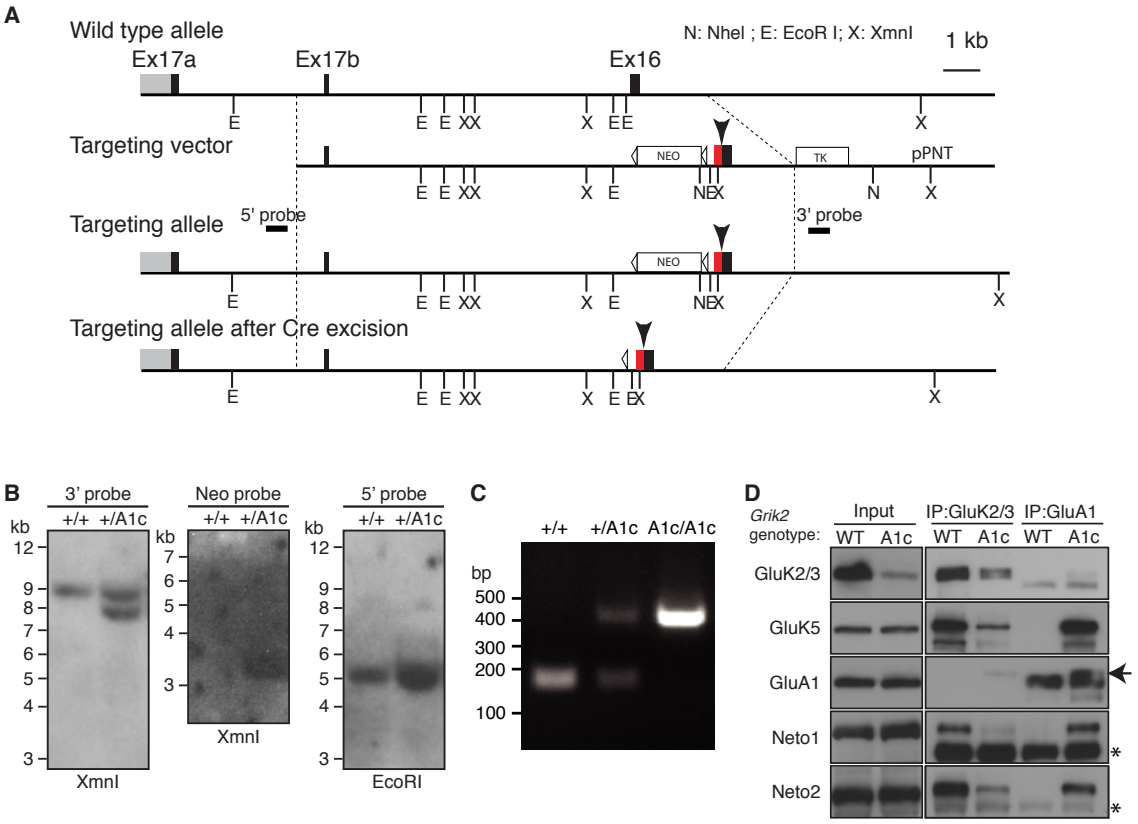

Figure S2. Generation of GluK2.A1c knock-in (KI) mice, Related to Figure 2

(A) Schematic representation of the genomic locus of the *Grik2* gene (encoding GluK2), targeting vector, targeted allele, and targeted allele after excision of the LoxP cassette. Red box indicates the inserted sequence encoding for the GluA1 cytoplasmic domain (243 bp) with two stop codons. *Grik2* encodes two alternative exon variants encoding two variants of the GluK2 C-terminus (exon 17a/b), and the strategy used here ensures expression of GluK2.A1cyto independent of these splice events. (B) Confirmation of homologous recombination by Southern blotting with probes shown in (A). (C) Example of genotyping PCR. +/+: wild type; +/A1: GluK2.A1c heterozygous; A1c/A1c: GluK2.A1c homozygous. (D) Protein interaction with GluK2 or GluK2.A1cyto was analyzed by co-immunoprecipitation using cerebral cortical lysate from wild-type (WT) and GluK2.A1c KI mice (A1c), using anti-GluK2/3 and -GluA1 antibodies that specifically recognize the respective cytoplasmic domains. GluK2.A1cyto was detected weakly at a slightly higher molecular weight than that of endogenous GluA1 (arrow). GluK5, Neto1 and Neto2 were co-immunoprecipitated efficiently by anti-GluK2/3 antibody in WT mice as well as by anti GluA1 antibody in GluK2.A1c KI mice. Asterisks indicate Ig heavy chains.

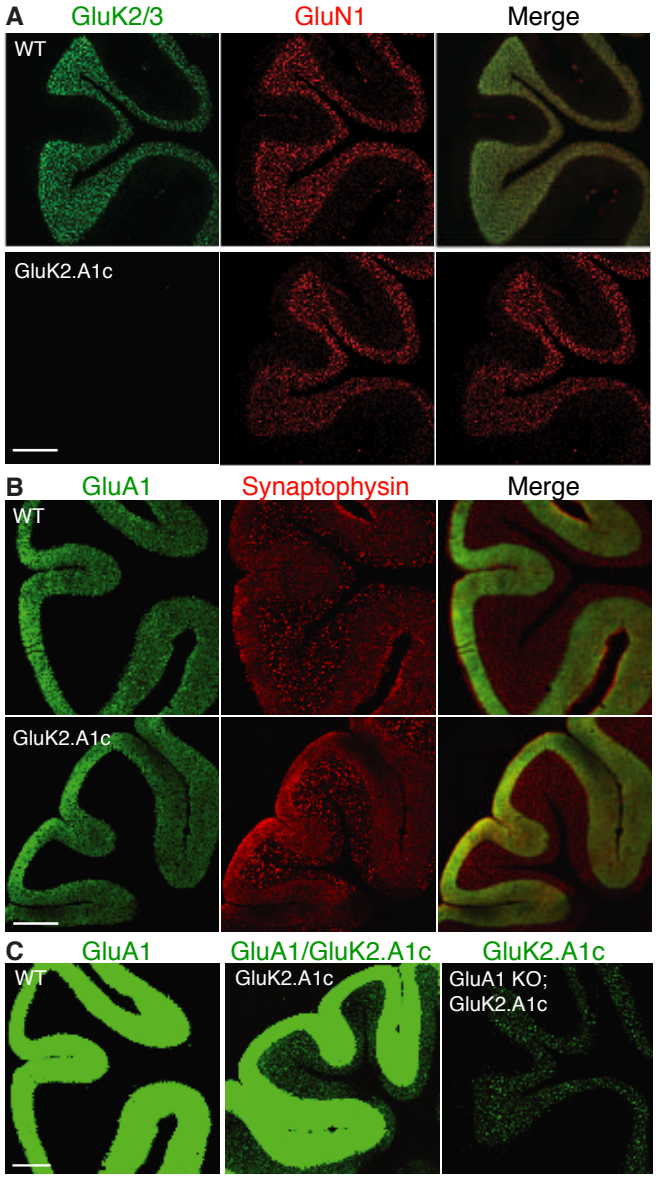

Figure S3. GluK2.A1cyto protein expression in the cerebellar granular layer, Related to Figure 3

(A) GluK2 signal was detected by anti-GluK2/3 antibody in wild-type (WT), but not in GluK2.A1c KI mice. GluN1 was used as a glomeruli postsynaptic marker. (B) Strong GluA1 signal was observed in the molecular layer of both WT and GluK2.A1c KI mice. Synaptophysin is used as a presynaptic marker. (C) A stronger exposure revealed an additional weak GluA1 signal, representing GluK2.A1cyto protein expression in the granular layer of GluK2.A1c KI mice, but not WT mice. Specific GluA1 signal was observed in the cerebellar granular layer of GluK2.A1c KI; GluA1 DKO mice. Scale bars: 200 μm.

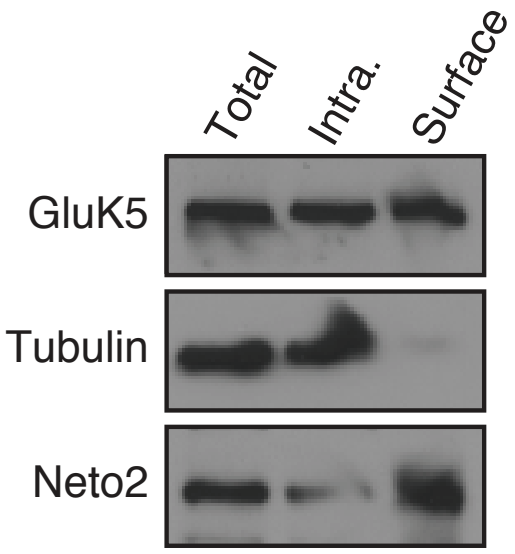

Figure S4. Specific detection of cell surface proteins using biotinylated reagents, Related to Figure 4

Acute hippocampal slices were prepared and biotinylated with cell-impermeable Sulfo-NHS-SS-biotin. After solubilization, biotinylated proteins were precipitated with Neutravidin-beads to isolate cell surface proteins. GluK5 and Neto2 were detected in the "Surface" fraction, whereas a cytosolic protein, tubulin, was detected in the "Internal" fraction. This suggests specific detection of cell surface proteins.

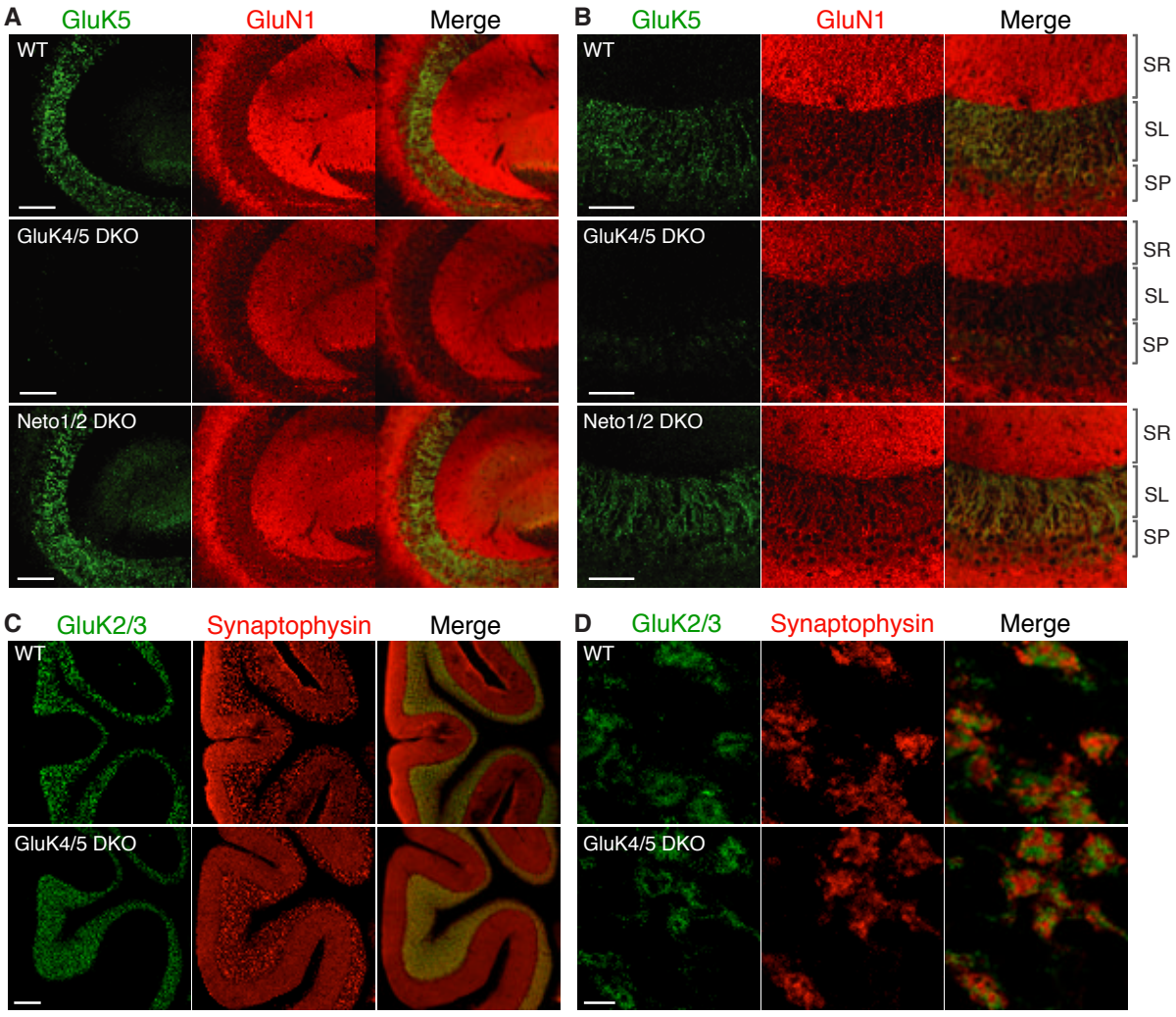

Figure S5. Localization of kainate receptors in hippocampus and cerebellum, Related to Figure 6

(A, B) In wild-type mice (WT), GluK5 localized at the stratum lucidum, similar to the distribution pattern observed for GluK2/3 (Fig. 6A, B). GluK5 signal was unaffected in Neto1/2 DKO mice, but abolished in GluK4/5 DKO mice. Images are shown at lower (A) and higher (B) magnifications. Scale bars: 100 μm (A), 50 μm (B). (C, D) GluK2 localized similarly in the granular layer of cerebellum in wild-type (WT) and GluK4/5 DKO mice, shown at lower (C) and higher (D) magnifications. Scale bars: 200 μm (C), 10 μm (D).

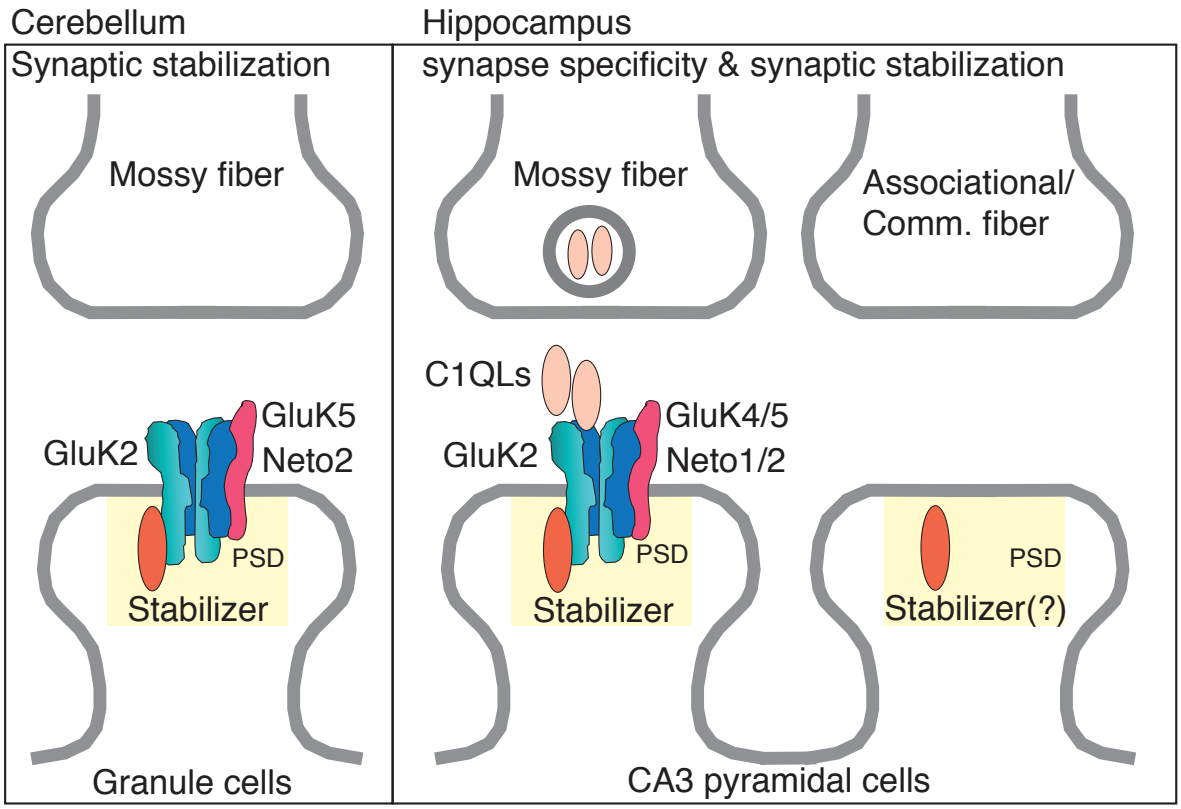

Figure S6. A model for synaptic localization of kainate receptors, Related to Figure 7

In the cerebellum, granule cells form only one type of excitatory synapses with mossy fibers, and kainate receptors require only synaptic stabilization mediated by the GluK2 cytoplasmic domain. In the hippocampus, CA3 pyramidal neurons form multiple distinct excitatory synapses and kainate receptors localize only at synapses with mossy fibers. In this situation, input-specific synaptic localization of kainate receptors requires both synaptic stabilization mediated by the GluK2 cytoplasmic domain and synapse-specific localization mediated by the GluK5 extracellular domain. The extracellular domain of GluK5 interacts with C1QLs released from mossy fiber terminals. The synaptic stabilizer that interacts with the GluK2 cytoplasmic domain remains unidentified.

Supplemental Experimental Procedure

Animals

All animal experiments were carried out in accordance with protocols approved by the Institutional Animal Care and Use Committees of both Yale University and Northwestern University, following guidelines described, in accordance with National Institutes of Health guidelines.

Generation of GluK2.A1cyto knock-in mice

A homologous recombineering technique was used to generate the targeting vector (Figure S2A). Mouse embryonic stem (ES) cells derived from C57BL/6J mice were transfected with DNA and selected by neomycin resistance. Upon confirmation of proper homologous recombination, ES cells were injected into mouse blastocysts by the Yale University Transgenic Mouse Service. Chimeric mice were identified by coat color and mated to Actin-Cre mice. Heterozygous male and female mice were subsequently mated to obtain homozygous knock-in mice. All mice were maintained at the Yale animal facility under the guidelines of the Institutional Animal Care and Use Committee.

Antibodies

The following antibodies were used: rabbit polyclonal antibodies to GluA1, GluA2/3, GluK2/3, and GluK5 (Millipore), mouse monoclonal antibodies to GluN1 (BD Biosciences), PSD-95, VGLUT1 (NeuroMab), synaptophysin (Sigma), and actin (Millipore), and rat anti-HA antibody (Roche). Rabbit polyclonal antibodies to Neto1 and Neto2 were described previously (Zhang *et al.*, 2009, Straub *et al*., 2011). Guinea pig polyclonal antibody to Neto1 was described previously (Straub *et al*., 2011).

Biochemical analysis

PSD fraction and co-immunoprecipitation were performed as described (Zhang *et al.*, 2009, Straub *et al*., 2011). Fractions were then analyzed by SDS-PAGE and western blotting, and samples were adjusted by protein amount.

Immunostaining

Under deep pentobarbital anesthesia (100 mg/kg of body weight, subcutaneous) mice were perfused transcardially with 4% paraformaldehyde (PFA) in 0.1 M phosphate buffer (PB), pH 7.4.. For immunohistochemistry, 40 μm free-floating sections were permeabilized (PBS/Triton-X 0.1%), blocked (PBS containing 3% normal goat serum), and incubated with primary antibodies. Final staining was performed using Alexa-conjugated secondary antibodies (Invitrogen). With the exception of Figure 6A-C and Figure 7, all immunohistochemistry experiments included an antigen retrieval step, by treating the sections with 1 mg/ml pepsin in 0.2 N HCl at 37°C prior to permeabilization. Images were acquired on a laser-scanning confocal microscope (Zeiss 710, or Zeiss 780).

Immuno-electron microscopy

For postembedding immunogold electron microscopy, microslicer slices (400 μm) were cryoprotected with 30% glycerol in PB, and frozen rapidly with liquid propane in the EM CPC unit (Leica Microsystems). Frozen sections were immersed in 0.5% uranyl acetate in methanol at -90˚C in the AFS freeze-substitution unit (Leica Microsystems), infiltrated at -45˚C with Lowicryl HM-20 resin (Electron Microscopy Sciences, Hatfield, PA), and polymerized with UV light. Ultrathin sections on nickel grids were etched with saturated sodium-ethanolate solution for 1-5 sec, and treated with following solutions: blocking solution containing 2% normal goat serum (Nichirei, Japan) in incubation solution (0.03% Triton-X100 in Tris-buffered saline, pH 7.4; TTBS) for 20 min, primary antibodies (20 μg/ml for each) diluted with the blocking solution overnight, and colloidal gold (10 nm)-conjugated anti-rabbit IgG (1:100, British BioCell International, UK) in the blocking solution for 2 hr. After extensive washing in TTBS and distilled water, sections were fixed with 1% OsO4 for 15 min and then stained with 5% uranyl acetate/40% EtOH for 90 s and Reynold's lead citrate solution for 60 s. Photographs were taken with an H-7100 electron microscope (Hitachi, Japan). For quantitative analysis, postsynaptic membrane-associated immunogold particles, being defined as those apart less than 35 nm from the cell membrane, were counted on scanned electron micrographs and analyzed using MetaMorph software (Molecular Devices).

Receptor surface expression and two-electrode voltage clamp in oocytes

Measurements of surface expression and activity of receptors expressed in oocytes were performed as described (Zhang *et al.*, 2009, Straub *et al*., 2011). cRNAs were produced with

T7 mMessage mMachine (Ambion), and injected into Xenopus laevis oocytes. 2-3 days after injection, glutamate-evoked currents were measured by two-electrode voltage clamp recording. For measurements of surface expression, oocytes expressing HA-tagged receptors were incubated with anti-HA antibody, followed by incubation with horseradish-peroxidase (HRP) tagged anti-rat antibody. HRP activity at the surface was measured by chemiluminescence with HRP-substrate (ELISA Femto Maximum Sensitivity, Pierce), using an automated plate reader (Wallac 1420, Perkin Elmer).

Electrophysiology - cerebellum

Whole cell recording of acute cerebellar slices was performed as described (Yan *et al*, 2013). Sagittal cerebellar slices with a thickness of 200 μm were prepared from P21–30 mice. Patch-clamp recordings from granule cells that were identified visually in cerebellar slices were performed on whole-cell mode. The resistance of patch pipettes was 5–10 MΩ when filled with intracellular solution. For voltage-clamp mode, the intracellular solution was composed of in (mM) 130 cesium methanesulfonate, 5 HEPES, 5 Mg-ATP, 0.2 Na-GTP, 20 TEA, and 5 EGTA, pH adjusted with CsOH to 7.3; and for current-clamp mode, the intracellular solution was composed of (in mM) 125 potassium gluconate, 20 KCl, 5 HEPES, 5 Mg-ATP, 0.2 Na-GTP, and 10 EGTA, pH adjusted with KOH to 7.3. The composition of the standard bathing solution was (in mM) 125 NaCl, 2.4 KCl, 2 $CaCl_2$, 1 $MgCl_2$, 1.2 NaH_2PO_4, 25 $NaHCO_3$, and 25 glucose; this solution was bubbled continuously with a mixture of 95% O_2 and 5% CO_2. Picrotoxin (100 μM) was always present in the saline solution to block spontaneous IPSCs. D-AP5 (50 μM) was used to block NMDA receptors, and GYKI53655 (30 μM) was used to block AMPA receptors. Stimulation and on-line data acquisition were performed using the Clampex program (version 10.2, Axon Instruments). Signals were filtered at 3 kHz and digitized at 20 kHz. Presynaptic mossy fibers were stimulated by placing a 5-10 μm micropipette in the granular layer and stimulating with 5-15 μA (A365 stimulus isolator; World Precision Instruments). Stimulation intensity was adjusted just above the sharp threshold for activation of the synaptic response with a holding potential at +40 mV. MF-EPSCs were recorded at -70 mV and corresponding MF-EPSPs were obtained by switching to current clamp mode. All recordings were performed at room temperature.

Electrophysiology - hippocampus

Horizontal slices from the ventral hippocampus (350 μm) were prepared from mice aged P19 – P27 as previously described (Fernandes et al., 2009). Briefly, animals were anesthetized with isoflurane and an intraperitoneal injection of ketamine/xylazine, and before decapitation. The brain was removed under ice-cold, sucrose based slicing solution containing: 85 NaCl, 2.5 KCl, 1.25 NaH_2PO_4, 25 $NaHCO_3$, 25 glucose, 75 sucrose, 0.5 $CaCl_2$, 4 $MgCl_2$, 0.5 ascorbic acid, 0.01 DL-APV, and 0.1 kynurenic acid (in mM), equilibrated with 95% O_2 and 5% CO_2. Slices were heated to 28.5°C before being returned to room temperature while slowly exchanging from slicing solution to ACSF containing the following (in mM): 125 NaCl, 2.4 KCl, 1.2 NaH2PO_4, 25 $NaHCO_3$, 25 glucose, 1 $CaCl_2$, 2 $MgCl_2$, 0.01 DL-APV, and 0.1 kynurenic acid. After at least 60 mins recovery slices were transferred to a recording chamber and continuously perfused with oxygenated ACSF for recordings containing 2 mM $CaCl_2$ and 1 mM $MgCl_2$. Recordings were performed at 30°C. For whole-cell voltage-clamp recordings, electrodes were manufactured from borosilicate glass pipettes. The resistance of the electrodes was 2.5– 4.5 MΩ when filled with an internal solution containing (in mM) 95 CsF, 25 CsCl, 10 Cs-HEPES, 10 Cs-EGTA, 2 NaCl, 2 Mg-ATP, 10 QX-314, 5 TEA-Cl, and 5 4-AP, pH adjusted to 7.3 with CsOH. Data were collected and analyzed using pClamp 10 software (Molecular Devices, Sunnyvale, CA). Series resistance was continuously monitored using hyperpolarizing voltage steps, and recordings were discarded if there was a >20% change during the experiment. MF synaptic currents were evoked using a monopolar glass electrode filled with ACSF positioned in the stratum lucidum. Criteria for acceptable MF-EPSCs were as previously reported (Armstrong et al., 2006; Contractor et al., 2001). EPSCs were isolated using the $GABA_A$ receptor antagonists, bicuculline (10 μM) and picrotoxin (50 μM), and NMDAR antagonist D-APV (50 μM). KAR mediated currents were isolated by inclusion of AMPAR antagonist GYKI53655 (50 μM) to the recording solution, and then confirmed by the inhibition by AMPAR / KAR antagonist CNQX (10 μM). Agonist-evoked currents were activated by bath application of 10 μM kainate in the presence of antagonists of AMPA, NMDA and $GABA_A$ receptors

Electrophysiology – Biophysics of receptors

Patch-clamp recordings of glutamate-evoked currents in outside-out patches were done at room temperature with an EPC-9 amplifier (HEKA) and PatchMaster acquisition software, essentially as described (Robert and Howe, 2003). The recordings were made at a holding potential of -100 mV. The external solution contained in mM: 150 NaCl, 3 KCl, 2 CaCl2, 1 MgCl2, 5 glucose and

10 HEPES (pH adjusted to 7.4 with NaOH). Patch pipettes (open tip resistance 4-10 MΩ) were filled with a solution containing in mM: 135 CsF, 33 CsOH, 2 MgCl2, 1 CaCl2, 11 EGTA and 10 HEPES (pH adjusted to 7.4 with CsOH). The external solution with and without glutamate (10 mM) was applied to the outside-out patch using theta glass pipettes mounted on a piezoelectric bimorph (Robert and Howe, 2003). Solution exchange times estimated from open tip potentials were 150-250 µs. The bath was superfused constantly with normal external solution at a rate of 1-2 ml/min (1 to 2 bath volumes per min). Glutamate (1 mM) was added to the external solution. Ensemble currents were low-pass filtered at 3 kHz and sampled at 20-50 kHz. For both deactivation (2 ms applications) and desensitization (300 ms applications), 30 trials were repeated at 8 s intervals and used to construct mean ensemble currents in PatchMaster (records that contained artifacts or jumps in the holding current were excluded). The mean records were exported to IGOR Pro software (Wavemetrics), and the decays of the currents were fitted with bi-exponential functions as described in Robert and Howe (2003). For deactivation, t = 0 was taken as the end of the 2 ms pulse of glutamate. For desensitization, the peak inward current was set to t = 0 before fitting. Between group comparisons of mean parameter values were made by two-way ANOVA with the on-line software package VassarStats.

Generation of GluK5 chimera constructs

Human GluK5 cDNA was C-terminally tagged with AcGFP (GluK5-GFP), followed by substitution of the GluK5 extracellular domain (S22 to S543), the GluK5 transmembrane domain (S543 to I827), or the GluK5 cytoplasmic domain (F826 to C-terminus) with their respective domains from GluK2. In addition, we deleted the GluK2 antigen site (HTFNDRRLPGKETMA) from the GluK5.K2cyto-GFP construct to allow selective labeling of endogenous GluK2 upon *in vivo* expression of the construct. For AAV generation, chimeras were cloned into a pAAV vector with synapsin promoter, and AAV was generated in 293AAV cells using the AAV-DJ system (Cell Biolabs). For surface expression assay in oocytes, HA tag was inserted at the N-terminus of the various constructs following GluK5 residue S22.

Stereotaxic surgery for AAV delivery *in vivo*

Adult mice (>6 weeks old) were anaesthetized with isoflurane and placed on a heated (37°C) stereotactic device. Recombinant AAV viruses were injected unilaterally to the hippocampal CA3 region using the following coordinates (relative to Bregma): 2.0, 1.85, 1.75 (X, Y, Z). At

>12 days post-injection, successful viral transduction was readily observed in coronal brain slices as a robust, unilateral GFP signal within the CA3 region of the affected hemisphere (see Fig. 7D). All subsequent histological analyses were confirmed using the non-injected hemisphere of the same animal as a negative control.

Statistical analysis

All data are given as the mean ± standard error of the mean (s.e.m.). Statistical significance was calculated using the unpaired Student's *t*-test or one-way ANOVA, as indicated.

REFERENCES

Armstrong, J.N., Saganich, M.J., Xu, N.J., Henkemeyer, M., Heinemann, S.F., and Contractor, A. (2006). B-ephrin reverse signaling is required for NMDA-independent long-term potentiation of mossy fibers in the hippocampus. J Neurosci 26, 3474-3481.

Contractor, A., Swanson, G., and Heinemann, S.F. (2001). Kainate receptors are involved in short- and long-term plasticity at mossy fiber synapses in the hippocampus. Neuron 29, 209-216.

Fernandes, H.B., Catches, J.S., Petralia, R.S., Copits, B.A., Xu, J., Russell, T.A., Swanson, G.T., and Contractor, A. (2009). High-affinity kainate receptor subunits are necessary for ionotropic but not metabotropic signaling. Neuron 63, 818-829.

Robert, A., and Howe, J.R. (2003). How AMPA receptor desensitization depends on receptor occupancy. J Neurosci 23, 847-858.